Oxidoreductase activity is necessary for N-glycosylation of cysteine-proximal acceptor sites in glycoproteins

Natalia A. Cherepanova, Shiteshu Shrimal, and Reid Gilmore

Department of Biochemistry and Molecular Pharmacology, University of Massachusetts Medical School, Worcester, MA 01605

Stabilization of protein tertiary structure by disulfides can interfere with glycosylation of acceptor sites (NXT/S) in nascent polypeptides. Here, we show that MagT1, an ER-localized thioredoxin homologue, is a subunit of the STT3B isoform of the oligosaccharyltransferase (OST). The lumenally oriented active site CVVC motif in MagT1 is required for glycosylation of STT3B-dependent acceptor sites including those that are closely bracketed by disulfides or contain cysteine as the internal residue (NCT/S). The MagT1- and STT3B-dependent glycosylation of cysteine-proximal acceptor sites can be reduced by eliminating cysteine residues. The predominant form of MagT1 in vivo is oxidized, which is consistent with transient formation of mixed disulfides between MagT1 and a glycoprotein substrate to facilitate access of STT3B to unmodified acceptor sites. Cotranslational N-glycosylation by the STT3A isoform of the OST, which lacks MagT1, allows efficient modification of acceptor sites in cysteine-rich protein domains before disulfide bond formation. Thus, mammalian cells use two mechanisms to achieve N-glycosylation of cysteine proximal acceptor sites.

Introduction

Asparagine-linked glycosylation of proteins in the lumen of the rough ER (RER) is an essential protein modification reaction in higher eukaryotes. Most consensus acceptor sites (NXT/S, sequons) are glycosylated by the oligosaccharyltransferase (OST) as the nascent polypeptide is passing through the protein translocation channel into the RER lumen. However, certain acceptor sites are modified by a posttranslocational pathway (Bolt et al., 2005; Ruiz-Canada et al., 2009; Shrimal et al., 2013b). A posttranslocational mode of glycan transfer poses a challenge to efficient glycosylation because protein-folding events, particularly disulfide bond formation, will stabilize protein secondary and tertiary structures that are incompatible with binding of the acceptor sequence to the OST active site (Kowarik et al., 2006; Lizak et al., 2011).

Most eukaryotic organisms assemble heterooligomeric OST complexes that consist of a catalytic subunit (an STT3 protein) plus three to seven accessory subunits (Kelleher and Gilmore, 2006). Metazoan organisms express two STT3 proteins (STT3A and STT3B) that are incorporated into distinct OST complexes that have partially overlapping roles in N-linked glycosylation (Kelleher et al., 2003; Ruiz-Canada et al., 2009; Shrimal et al., 2013b). The STT3A complex is associated with the protein translocation channel and glycosylates acceptor sites as they enter the lumen of the RER (Nilsson et al., 2003; Shibatani et al., 2005; Ruiz-Canada et al., 2009), whereas the STT3B complex can modify sites that are skipped by STT3A (Ruiz-Canada et al., 2009; Shrimal et al., 2013b). In addition to a shared set of noncatalytic subunits (ribophorin I, ribophorin II, OST48, DAD1, and OST4) that are present in both OST complexes (Kelleher et al., 2003; Dumax-Vorzet et al., 2013), there is a growing list of OST-associated proteins or subunits (MagT1, TUSC3, DC2, KPC2, and malectin) that in some cases are

Correspondence to Reid Gilmore: reid.gilmore@umassmed.edu

Abbreviations used in this paper: ARMR, autosomal-recessive mental retardation; β-GUS, β-glucuronidase; CDG-1, congenital disorders of glycosylation type 1; co-IP, coimmunoprecipitation; cRM, canine pancreas rough microsomal membranes; DPS, dipyridyl disulfide; DTT, dithiothreitol; EH, endoglycosidase H; Hpx, hemopexin; LC-MS/MS, liquid chromatography–tandem mass spectrometry; NC, negative control siRNA; NEM, *N*-ethyl maleimide; OST, oligosaccharyltransferase; pCatC, procathepsin C; PDI, protein disulfide isomerase; RER, rough ER; SHBG, sex hormone binding globulin; XLMR, X-linked mental retardation.

The Rockefeller University Press $30.00
J. Cell Biol. Vol. 206 No. 4 525–539
www.jcb.org/cgi/doi/10.1083/jcb.201404083

isoform specific (Shibatani et al., 2005; Qin et al., 2012; Roboti and High, 2012).

Two mammalian proteins, currently annotated as magnesium transporter 1 (MagT1; formerly IAP) and tumor suppressor candidate 3 (TUSC3; formerly N33) were initially proposed to be OST subunits based upon homology to the yeast Ost3 and Ost6 proteins (MacGrogan et al., 1996; Kelleher et al., 2003). The mechanistic role of MagT1 and TUSC3 in protein N-glycosylation has been difficult to biochemically evaluate as these proteins dissociate from the canine OST during purification and are dispensable for glycosylation of synthetic peptide substrates (Kelleher et al., 2003). Despite the modest sequence identity (~20%) between yeast Ost3/Ost6 and either TUSC3 or MagT1, the four proteins share a lumenally oriented thioredoxin domain followed by four transmembrane spans (Fetrow et al., 2001; Kelleher and Gilmore, 2006). Mutagenesis of the active site CXXC motifs in Ost3 or Ost6 reduces glycan occupancy on specific acceptor sites in yeast glycoproteins (Schulz et al., 2009). The lumenal domains of Ost6p and TUSC3, both of which have a strongly negative redox potential, have been crystalized, which confirms the predicted thioredoxin fold (Schulz et al., 2009; Mohorko et al., 2014).

MagT1 and TUSC3 have also been proposed to be plasma membrane localized magnesium transporters (Goytain and Quamme, 2005). Multiple lines of experimental evidence support the conclusion that MagT1 and TUSC3 are required for magnesium uptake by vertebrate cells (Zhou and Clapham, 2009). However, overexpression of MagT1 alone does not increase the Mg^{2+} concentration in cells even though MagT1, but not TUSC3, is expressed in most human tissues (Molinari et al., 2008; Zhou and Clapham, 2009). MagT1-deficient human lymphocytes display altered kinetics of Mg^{2+} uptake, but have normal cellular levels of Mg^{2+} (Li et al., 2011).

Mutations in the human *TUSC3* gene cause autosomal-recessive mental retardation (ARMR), a disease primarily characterized by mental impairment (Garshasbi et al., 2008; Molinari et al., 2008). Mutations in the *MAGT1* gene cause X-linked mental retardation (XLMR; Molinari et al., 2008) and X-linked human immunodeficiency syndrome (Li et al., 2011). Analysis of serum glycoproteins from TUSC3 patients has not disclosed any defect in protein N-glycosylation (Molinari et al., 2008), further challenging a direct role for TUSC3 or MagT1 in N-glycosylation.

Here, we show that MagT1 colocalizes with calreticulin, a lumenal lectin in the RER. We explored the hypothesis that MagT1 is required for efficient glycosylation of certain human glycoproteins. siRNA-mediated depletion of MagT1 reduced glycan occupancy on a panel of STT3B-dependent substrates, which is consistent with native co-IP experiments showing that MagT1 is a subunit of the STT3B complex. Inspection of MagT1-dependent acceptor sites in proteins of known tertiary structure revealed that many MagT1-dependent sites were either closely bracketed by a disulfide or that the sequon contained a disulfide-bonded cysteine as the X residue (i.e., NCT/S sites). The MagT1 dependence of glycosylation was reduced by eliminating sequon-proximal cysteine residues or by reducing the ER lumen with DTT. MagT1-depleted cells were fully complemented by expression of TUSC3, which is indicative of functional redundancy between MagT1 and TUSC3. In the cell, the majority of MagT1 is in the oxidized state. Therefore, MagT1 can form a transient mixed disulfide with a free thiol in a glycoprotein substrate, thereby delaying disulfide bond formation until STT3B glycosylates the acceptor site. The reduced form of MagT1 can react with a disulfide in a nascent polypeptide to allow access of STT3B to an inaccessible sequon.

Results

MagT1 resides in the ER

Direct roles for MagT1 in both N-linked glycosylation and magnesium uptake are incompatible unless one invokes both a dual localization (RER and plasma membrane) and a dual activity (oxidoreductase and Mg^{+2} channel). Intact HeLa cells were treated with a membrane impermeable amine-reactive biotinylation reagent to label cell surface proteins. Biotinylated proteins that were collected on streptavidin beads were electrophoresed adjacent to an aliquot of the total HeLa cell extract to quantify the percentage of each antigen that was accessible to the biotinylation reagent (Fig. 1 A). The plasma membrane Na^+K^+-ATPase was strongly enriched in the streptavidin-bound fraction relative to the α subunit of the F_0F_1-ATPase, a mitochondrial protein that served as the negative control. MagT1 and two subunits of the OST (STT3B and ribophorin I) showed very low reactivity with Sulfo-NHS-SS-Biotin, which is consistent with an intracellular localization. Broken cells likely account for the 2–3% of intracellular proteins that were recovered on the streptavidin beads.

Immunofluorescence microscopy of permeabilized cells showed a reticular staining pattern for endogenous MagT1 that surrounds the nucleus and does not colocalize with the Na^+K^+-ATPase (Fig. 1 B, a–c). HeLa cells were transfected with an expression vector for MagT1-V5 to allow simultaneous staining for MagT1-V5 and the luminal ER protein calreticulin (Fig. 1 B, d–f). Colocalization of MagT1-V5 and calreticulin confirmed that MagT1 is an ER resident protein.

MagT1 depletion reduces glycosylation of STT3B-dependent substrates

siRNA duplexes were designed to explore a role for MagT1 in N-linked glycosylation. HeLa cells treated with MagT1 siRNA typically showed a two- to threefold reduction in MagT1 content after 72 h (Fig. 2 A). Expression of STT3A, STT3B, ribophorin I, or the protein translocation channel (Sec61) was not reduced by treatment with the MagT1 siRNA. In contrast, depletion of STT3B was accompanied by a marked reduction in MagT1 expression (Fig. 2 A). Mutations in the human STT3A and STT3B genes cause two newly described forms of congenital disorders of glycosylation type 1 (CDG-1; Shrimal et al., 2013a). Protein immunoblot analysis revealed that STT3B-CDG fibroblasts have a lower cellular content of both STT3B and MagT1 relative to STT3A-CDG fibroblasts or normal control fibroblasts (Fig. 2 B), providing additional evidence that stable expression of MagT1 is dependent on STT3B.

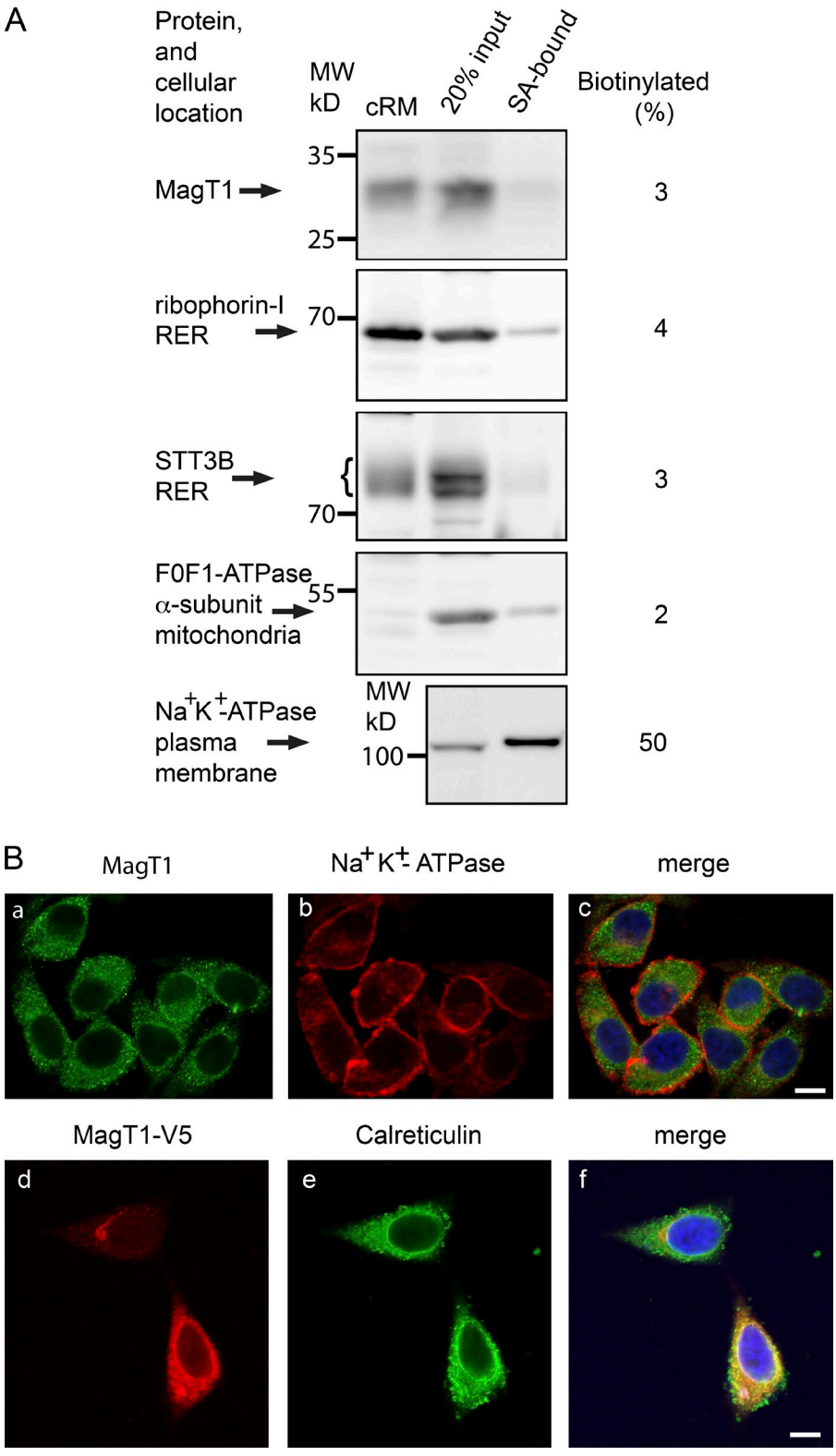

Figure 1. **MagT1 is localized to the RER.** (A) Cell-surface proteins labeled with sulfo-NHS-SS-biotin were isolated with streptavidin beads (SA-bound) and were resolved adjacent to sample input lanes by SDS-PAGE. The percentage of biotinylated protein was calculated as described in the Materials and methods. Canine pancreas RER membranes (cRM) were included as protein mobility standards for ER localized proteins. The indicated molecular weights shown in all figures are of prestained molecular weight markers electrophoresed on all gels. (B, a–c) HeLa cells were cultured for 24 h, fixed, and stained with antibodies to MagT1 (a and c, green) and the Na^+K^+-ATPase (b and c, red). (B, d–f) 24 h after transfection of HeLa cells with the MagT1-V5His expression vector, cells were fixed and stained with antibody against the V5 epitope (d and f, red) and calreticulin (e and f, green). The merged images (c and f) include the DAPI stain of the nucleus. Bars, 10 µm.

We next asked whether MagT1 depletion causes a reduction in N-glycosylation of newly synthesized proteins. For this analysis, we used a panel of substrates that have acceptor sites that are mainly glycosylated by either the STT3A or STT3B complex (Fig. 2, C–F). The two extreme C-terminal sequons in sex hormone binding globulin (SHBG) are posttranslocationally glycosylated by STT3B (Shrimal et al., 2013b). A diagram of SHBG (Fig. S1 D) shows the location of acceptor sites and cysteine residues. After 48 h of siRNA treatment, HeLa cells were transfected with an SHBG expression vector and pulse labeled 24 h later. Incomplete modification of the $N_{380}RS$ site in SHBG is responsible for the glycoform doublet synthesized

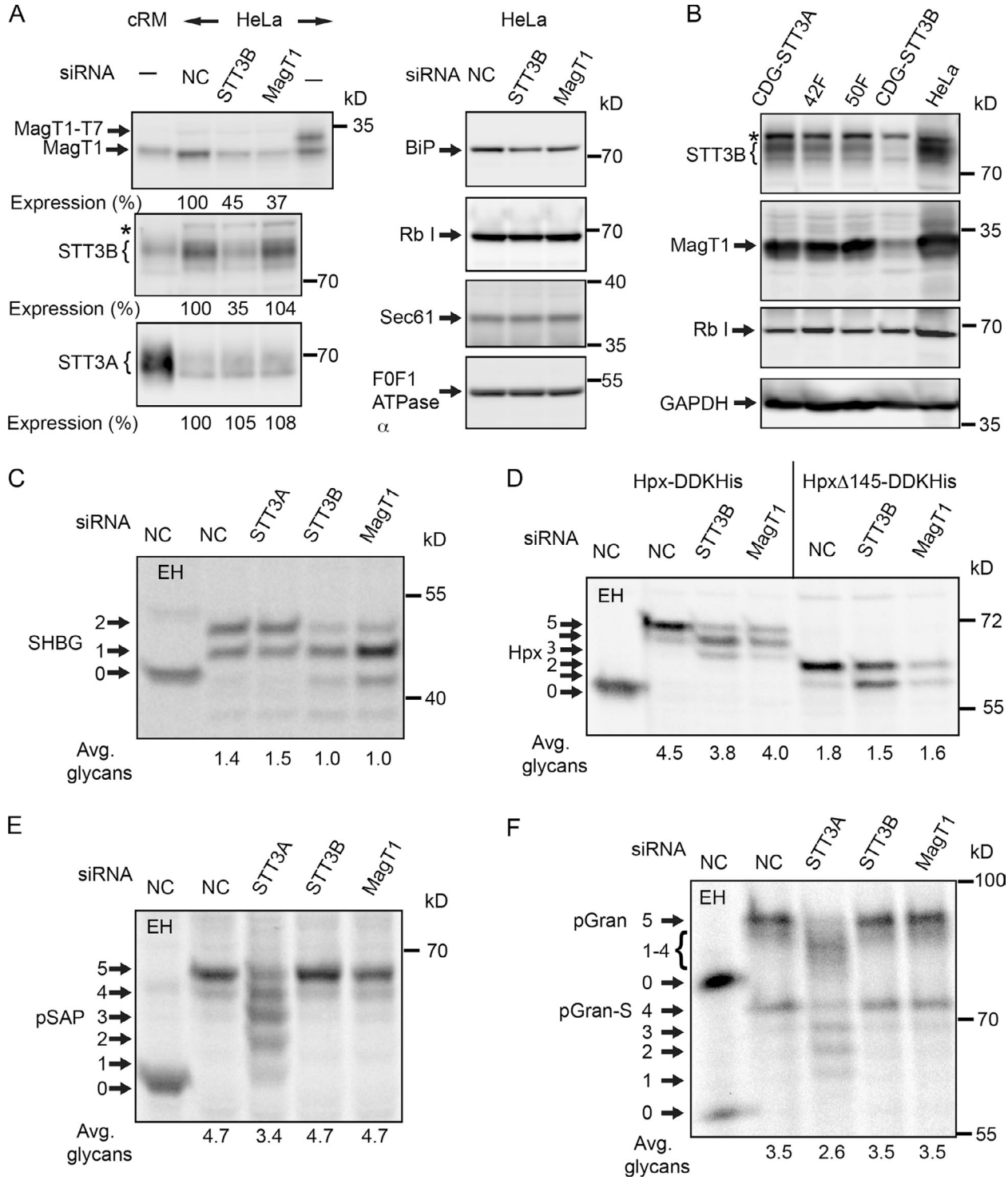

Figure 2. **Hypoglycosylation of STT3B-dependent substrates in MagT1-depleted cells.** (A and C–F) HeLa cells were treated with NC or siRNAs specific for STT3A, STT3B, or MagT1 for 72 h. (A) HeLa cell extracts and cRM were resolved by PAGE in SDS and analyzed by protein immunoblotting using the specified antisera. MagT1-T7 expressed in HeLa cells verified recognition of MagT1 by the anti-MagT1 sera. Expression values relative to cells treated with the NC siRNA are for the displayed image, which is representative of two or more experiments. (B) Cell extracts prepared from STT3A-CDG, STT3B-CDG, and normal control (42F and 50F) fibroblasts were resolved by PAGE in SDS and analyzed by protein immunoblotting. The F0F1-ATPase α (A) and glyceraldehyde 3-phosphate dehydrogenase (GAPDH; B) served as gel loading controls. The asterisks in A and B designate a nonspecific product recognized by the anti-STT3B sera. Protein expression levels for OST subunits were normalized to the F_0F_1-ATPase α subunit loading control and are expressed relative to the NC siRNA lane. (C–F) After 48 h of siRNA treatment, cells were transfected with expression vectors for SHBG (C), or Hpx (Hpx-DDKHis or HpxΔ145-DDKHis; D) and pulse-chase labeled (4 min pulse, 20 min chase) after an additional 24 h. (E and F) After 72 h of siRNA treatment, cells were pulse labeled for 4 min and chased for 10 min. As indicated, samples were digested with EH after immunoprecipitation with anti-SHBG (C), anti-DDK (D), anti-SapD (E), or anti-granulin (F). Glycoforms resolved by PAGE in SDS are labeled to indicate the number of N-linked glycans. EH-digested proteins migrate slightly slower than the nonglycosylated protein because of the presence of a single residual GlcNAc residue at each site. Quantified values below gel lanes (C–F) are for the displayed image, which is representative of two or more experiments.

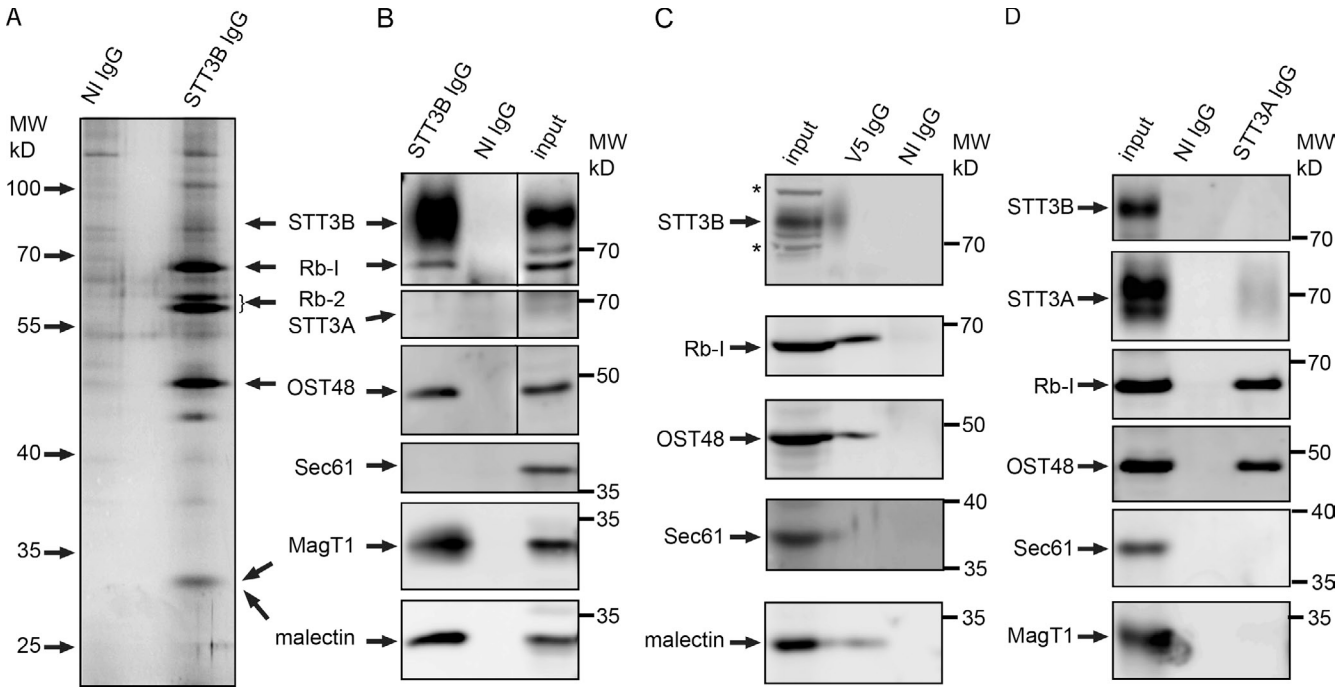

Figure 3. **MagT1 is a subunit of the STT3B complex.** (A, B, and D) cRM were solubilized under nondenaturing conditions and incubated with protein A–Sepharose beads with covalently coupled nonimmune (NI) IgG or anti-STT3B IgG (A and B) or noncoupled anti-STT3A IgG (D, anti-ITM1 sera). (C) HeLa cells expressing MagT1-V5 were solubilized and incubated with protein A–Sepharose beads coated with anti-V5 IgG or NI IgG. (A–D) Proteins were eluted with IP wash buffer, resolved by SDS-PAGE, and stained with silver (A) to detect major proteins including known OST subunits (STT3B, ribophorin I [Rb-1], ribophorin II [Rb-II], and OST48) or analyzed by protein immunoblotting using the indicated antisera (B–D). (B–D) Input samples (cRM [B and D] or HeLa cell extract [C]) were electrophoresed on the same gel to provide protein mobility markers. MagT1 and malectin co-migrate (B) with the 34-kD band detected by silver staining (A). Asterisks designate nonspecific bands recognized by the anti-STT3B sera on protein blots of the input samples. In B, vertical lines indicate removal of an intervening lane of molecular weight markers.

by control cells (Shrimal et al., 2013b). Endoglycosidase H (EH) digestion provides a mobility marker for the nonglycosylated protein. MagT1 or STT3B depletion caused a similar reduction in glycosylation of SHBG (Fig. 2 C). The partial block in glycosylation of SHBG in siRNA-treated cells is primarily explained by the incomplete depletion of STT3B or MagT1. Hemopexin (Hpx; Fig. S1 C) has five glycosylation sites including internal (N_{187}CS) and C-terminal (N_{453}VT) STT3B-dependent acceptor sites (Shrimal and Gilmore, 2013). Depletion of MagT1 or STT3B caused the synthesis of Hpx glycoforms that lack one or two glycans (Fig. 2 D). Cells were transfected with the HpxΔ145 construct, which retains the internal STT3B-dependent site and an STT3B-independent site (N_{240}GT). Glycosylation of the (N_{187}CS) site requires MagT1 in addition to STT3B. MagT1 was also required for glycosylation of the extreme C-terminal sequon in β-glucuronidase (β-GUS; Fig. S2, A and B). Prosaposin (pSAP; Fig. S1 A) and progranulin (pGran; Fig. S1 B) are endogenous HeLa cell STT3A-dependent substrates (Ruiz-Canada et al., 2009; Shrimal et al., 2013a). Prosaposin is hypoglycosylated in STT3A-depleted cells, but not in STT3B- or MagT1-depleted cells (Fig. 2 E). Serendipitous proteolytic processing of progranulin at a granulin repeat boundary in the cell lysis buffer yields a more rapidly migrating form of progranulin (pGran-S) with resolution of the granulin glycoforms (Fig. 2 F). MagT1 or STT3B depletion does not cause hypoglycosylation of granulin.

MagT1 is a subunit of the STT3B complex

Whereas Magt1 depletion caused selective hypoglycosylation of STT3B-dependent acceptor sites, we conducted native coimmunoprecipitation (co-IP) experiments to determine whether MagT1 is present in the STT3B complex, but not the STT3A complex. Canine pancreas microsomal membranes were solubilized with the nonionic detergent digitonin and incubated with anti-STT3B IgG or control IgG beads. Proteins that interact with STT3B were selectively eluted with an immunoprecipitation wash buffer containing mixed detergent micelles (1% Triton X-100, 0.1% SDS) instead of digitonin. The major eluted proteins that were detected by silver staining (Fig. 3 A) include the previously identified OST subunits (STT3B, ribophorin I, ribophorin II, and OST48), as confirmed by protein immunoblotting (Fig. 3 B) and liquid chromatography–tandem mass spectrometry (LC-MS/MS; Table 1). High peptide coverages were obtained for Rb-I, Rb-II, OST48, DADI, and malectin, with somewhat lower peptide coverage for proteins with multiple transmembrane spans (STT3B and MagT1). The 34-kD protein detected by silver staining (Fig. 3 A) comigrates with both MagT1 and malectin (Fig. 3 B). Malectin is an ER-localized lectin that recognizes the terminal Glc α,1-3 Glc disaccharide on the first trimming intermediate ($GlcNAc_2Man_9Glc_2$) of an N-linked oligosaccharide (Schallus et al., 2008; Schallus et al., 2010). Malectin is proposed to interact with ribophorin I (Qin et al., 2012). Similar LC-MS/MS results were obtained when HeLa cell extracts

Table 1. **Identification of proteins by LC-MS/MS in co-IP experiments**

Protein[a]	Peptide coverage[b]			
	STT3B[c]		STT3A[c]	MagT1-V5[c]
	cRM[d]	HeLa[d]	cRM[d]	HeLa[d]
STT3B	13	9	0	18
STT3A	0	0	3	0
Ribophorin I	75	42	47	39
Ribophorin II	58	37	13	44
OST48	53	44	43	40
MagT1	17	6	0	19
DAD1	35	19	19	19
Malectin	36	13	9	40
Calnexin[e]	10	0	0	22
Calreticulin[e]	0	0	0	34
Sec61α	0	0	0	0

[a]OST subunits that were not detected in any sample include TUSC3, OST4, DC2, and KPC2. OST4, DC2, and KPC2 are low molecular weight hydrophobic membrane proteins, so they may not have been detected due to the limited number of tryptic fragments. TUSC3 is not expressed in HeLa cells.
[b]Peptide coverage for the protein recognized by the precipitating antibody is low because the beads were eluted with a mixed-micelle immunoprecipitation wash buffer.
[c]Antibody.
[d]Membrane source. Digitonin solubilized HeLa cells or cRM were used for co-IP assays.
[e]The presence of calnexin and calreticulin in co-IP samples could not be verified by protein immunoblotting.

were used as the starting material for a native STT3B co-IP experiment (Table 1).

To provide additional evidence that MagT1 is associated with the STT3B complex, we expressed MagT1-V5 in HeLa cells and performed native co-IP experiments using anti-V5 sera. Protein immunoblots (Fig. 3 C) and LC-MS/MS analysis (Table 1) revealed that STT3B, Rb-I, Rb-II, OST48, DAD1, and malectin coimmunoprecipitate with MagT1-V5. Native co-IP experiments using antisera to STT3A and canine microsomes as the protein source yielded an STT3A complex (STT3A, Rb-I, Rb-II, OST48, DAD1, and malectin) that lacks STT3B and MagT1 (Fig. 3 D and Table 1). The interaction between the STT3A complex and Sec61 (Shibatani et al., 2005) is apparently not robust enough to detect in our co-IP assays.

Cysteine residues near MagT1-dependent sequons

Do STT3B-dependent glycosylation sites share features that mandate a role for MagT1? Previously identified STT3B-dependent glycosylation sites can be grouped into three categories: (1) extreme C-terminal sequons, (2) internal sequons (NXT/S) that are closely bracketed by a disulfide in the folded protein, and (3) internal NCT/S sequons where the cysteine residue is disulfide bonded in the mature protein. The STT3B dependence of extreme C-terminal acceptor sites is not explained by the presence of nearby disulfides or cysteine residues in the folded protein (Fig. S2).

Procathepsin C (pCatC; Fig. S1 E) has two NCT/S sites, one of which (N_{29}CT) is mainly glycosylated by the STT3B complex before nascent chain termination (Ruiz-Canada et al., 2009). HeLa cells were pulse labeled after a 5-min preincubation with the cell-permeable reducing agent DTT to determine whether the MagT1 dependence of pCatC glycosylation correlates with the oxidizing conditions that favor disulfide bond formation. Endogenous pCatC was hypoglycosylated in MagT1-depleted cells unless the ER lumen was reduced with DTT (Fig. 4 A). Further analysis of N_{29}CT glycosylation used the pCatCΔ234-HA expression vector that only retains the N_{29}CT site (Fig. 4 B). Glycosylation of the N_{29}CT sequon in pCatCΔ234-HA was reduced in STT3B- or MagT1-depleted cells unless formation of the C30-C118 disulfide was blocked by mutagenesis of the cysteine residues (Fig. 4 C). Thus, MagT1- and STT3B-dependent glycosylation of the N_{29}CT site correlates with the ability of C30 to form a disulfide.

Factor VII contains a glycosylation site (N_{360}IT) that is mainly posttranslocationally glycosylated by STT3B (Ruiz-Canada et al., 2009). Glycosylation of the N_{360}IT site was compared in FVII derivatives that cannot form the C348-C367 disulfide (Fig. 4 D). Elimination of the cysteine residues increased glycosylation of the N_{360}IT site in control or STT3A-depleted cells and reduced, but did not eliminate, the dependence upon STT3B and MagT1 (Fig. 4 E). Additional pulse-chase experiments were conducted using untreated cells to better understand how C348 and C367 influence the kinetics of glycosylation of the N_{360}IT site (Fig. 4 F). Replacement of the proximal cysteine residues increased the percentage of factor VII that was glycosylated during the pulse, and accelerated the rate and increased the extent of posttranslocational glycosylation. Thus, the cysteine residues flanking the sequon contribute to the slow posttranslocational modification of the N_{360}IT sequon by the STT3B complex, but they do not cause the N_{360}IT site to be skipped at a high frequency by the STT3A complex.

Active site disulfide in MagT1 and TUSC3

Human MagT1 and TUSC3 are 73% identical in sequence in the mature region of the protein and have thioredoxin CXXC motifs that are distinct from the CGHC motif in protein disulfide isomerase (PDI) family members (Fig. 5 A). Wild-type or

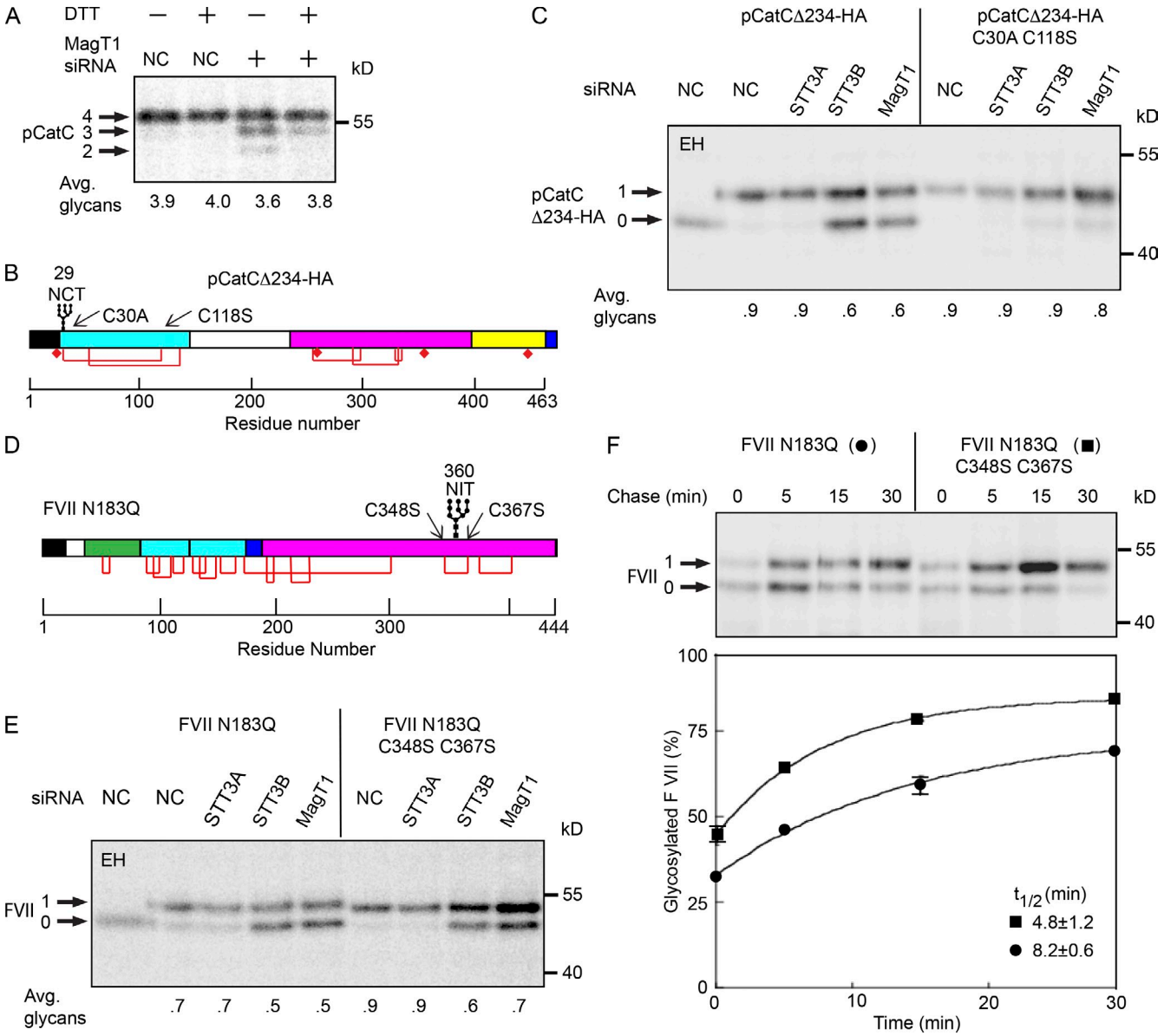

Figure 4. **Disulfide bonds in MagT1-dependent substrates.** (A) HeLa cells treated with NC or MagT1 siRNA were treated with 3 mM DTT for 5 min before a 5-min pulse, 10-min chase labeling period. Endogenous cathepsin C was immunoprecipitated using anti-CatC sera and resolved by SDS-PAGE. Diagrams of pCatCΔ234-HA (B) and FVII N183Q (D) showing the signal sequence (black), glycosylation sites, disulfide bonds (red lines), free cysteine residues (diamonds), mature protein domains (green, cyan, magenta, and yellow segments), and the C-terminal HA tag on pCatCΔ234-HA. Disulfides that link (pCatCΔ234) or bracket (FVII N183Q) a STT3B-dependent glycosylation site are indicated. (C and E) HeLa cells were treated with NC, or siRNAs specific for STT3A, STT3B, or MagT1 for 48 h as indicated, then transfected with pCatCΔ234-HA (C) or FVII N183Q (E and F) expression vectors and cultured for an additional 24 h before pulse labeling. Cells were pulse labeled for 4 min (C), pulse labeled for 2 min, and chased for 30 min (E), or pulsed for 2 min and chased as indicated (F). Glycoprotein substrates were precipitated with anti-HA sera (C) or anti-factor VII sera (E and F). Quantified values below gel lanes (A, C, and E) are for the displayed image that is representative of two or more experiments. Data points in F are the mean of two determinations, with individual data points indicated by error bars.

mutant forms of TUSC3 and MagT1 were expressed in MagT1-depleted cells to determine whether the CXXC motifs are important, and to test whether TUSC3 can replace MagT1 to promote glycosylation of pCatCΔ234-HA (Fig. 5 B). The siRNA target sequence in the MagT1 expression vector was altered to render the mRNA resistant to the MagT1 siRNA. Glycosylation of pCatCΔ234-HA was fully restored when the siRNA-treated cells were transfected with a wild-type MagT1 or TUSC3 expression vector (Fig. 5 B, top). Mutants that lacked both active site cysteine residues (e.g., MagT1 m1) were not able to fully restore glycosylation of pCatCΔ234-HA, which indicates that the CXXC motif is necessary for MagT1 and TUSC3 activity. Overexpression of STT3B-DDK could not compensate for depletion of MagT1. The partial restoration of glycosylation that is provided by the MagT1 m1 or TUSC3 m1 mutants indicates that MagT1 or TUSC3 is needed for both oxidoreductase-dependent and -independent functions of the STT3B complex.

Cell extracts were analyzed by protein immunoblotting to verify expression of MagT1-V5, TUSC3-DDK, and STT3B-DDK in the MagT1-depleted cells (Fig. 5 B). Because of the high

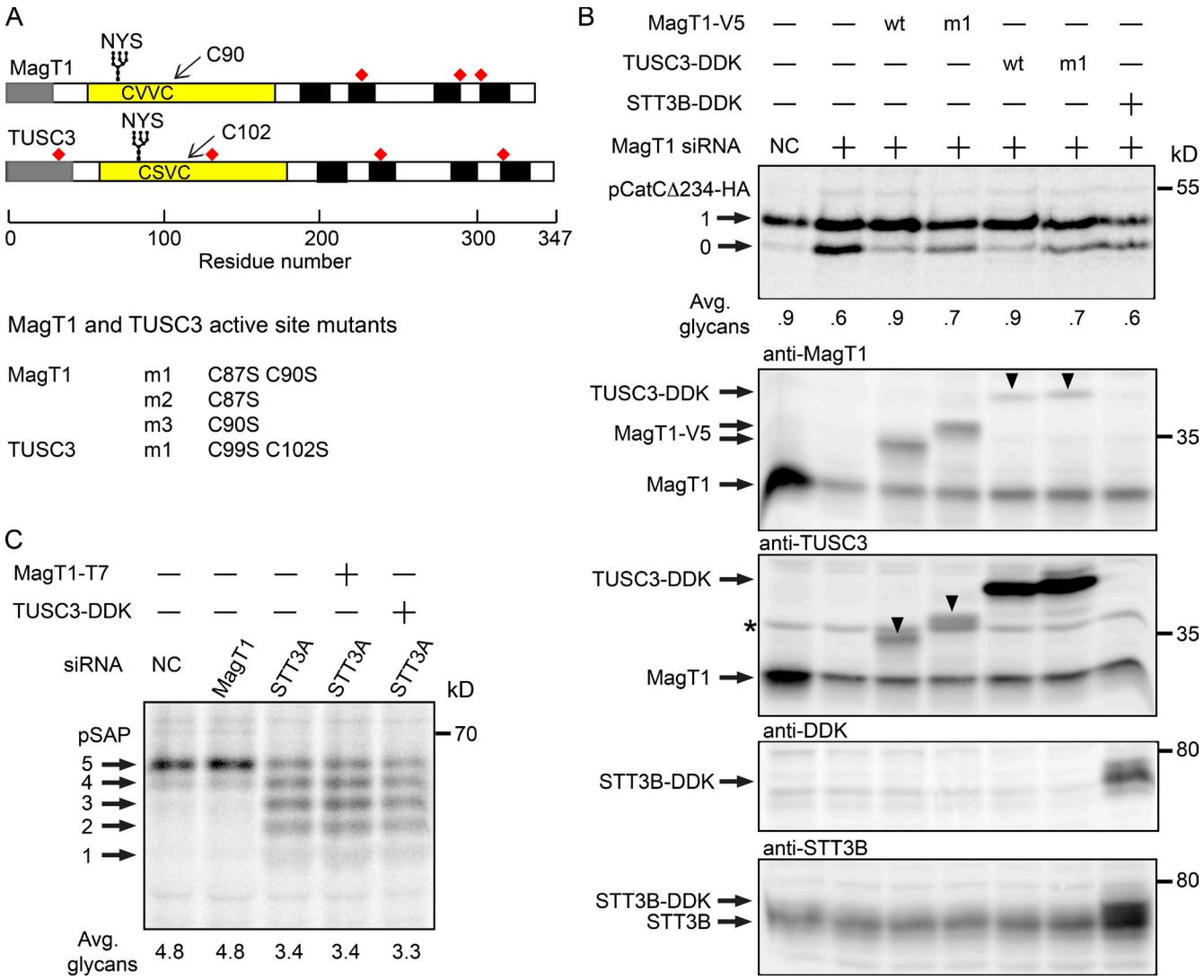

Figure 5. **Requirement for active site cysteine residues in MagT1 and TUSC3.** (A) Diagrams of MagT1 and TUSC3 showing the N-terminal signal sequence (gray), lumenal thioredoxin domain (yellow) with active-site CXXC motif, glycosylation site, noncatalytic cysteine residues (red squares), and membrane spanning segments (black). Nomenclature for single and double cysteine mutants of MagT1 and TUSC3 is given. (B) HeLa cells were treated with NC or MagT1 siRNA for 48 h before cotransfection with a pCatCΔ234-HA expression vector and a wild-type or mutant MagT1-V5, TUSC3-DDK, or STT3B-DDK expression vector. Cells were pulse labeled for 4 min and chased for 10 min. Glycoforms of CatCΔ234-HA were collected by immunoprecipitation with anti-HA and resolved by PAGE in SDS. Total protein extracts from cells were resolved by SDS-PAGE and analyzed by protein immunoblotting using anti-MagT1, anti-TUSC3, anti-DDK, and anti-STT3B sera. Downward pointing arrowheads in the anti-MagT1 and anti-TUSC3 blots designate cross-reaction with TUSC3-DDK and MagT1-V5, respectively. The band designated by the asterisk is not TUSC3, but is a nonspecific background protein (see Fig. S2 B). (C) HeLa cells treated for 48 h with NC, STT3A siRNA, or MagT1 siRNA were transfected with MagT1-T7 or TUSC3-DDK expression vectors as indicated 24 h before pulse labeling for 4 min and chase for 10 min. Prosaposin glycoforms were immunoprecipitated using anti–saposin D sera and resolved by SDS-PAGE. Quantified values below gel lanes (B and C) are for the displayed image that is representative of two experiments.

sequence identity between MagT1 and TUSC3, the commercially available MagT1 and TUSC3 antisera that we have tested show detectable cross-reactivity. TUSC3-DDK and MagT1-V5 were well resolved from endogenous MagT1, as detected using the anti-MagT1 or anti-TUSC3 sera. The protein designated by an asterisk in the anti-TUSC3 blot is a nonspecific background band based upon insensitivity to TUSC3 siRNA (Fig. S3 A) and failure to coprecipitate with STT3B, unlike TUSC3-DDK (Fig. S3 B). If present at all, endogenous TUSC3 is below the detection limits of the anti-TUSC3 sera. Overexpression of STT3B-DDK in the MagT1-depleted cells was detected using antibodies specific for the DDK epitope tag and STT3B (Fig. 5 B). Overexpression of MagT1-V5 or TUSC3-DDK does not restore glycosylation of prosaposin in STT3A-depleted cells (Fig. 5 C), and so the thioredoxin homologues do not indirectly enhance glycosylation of proteins in the ER.

Formation of mixed disulfides between MagT1 and glycoprotein substrates

The second glycosylation site in cathepsin C ($N_{53}CS$) is efficiently glycosylated in STT3B-depleted cells (Ruiz-Canada et al., 2009) despite the presence of an internal cysteine residue that is disulfide bonded in the mature protein. Why is the STT3B complex required for glycosylation of the first, but not the second,

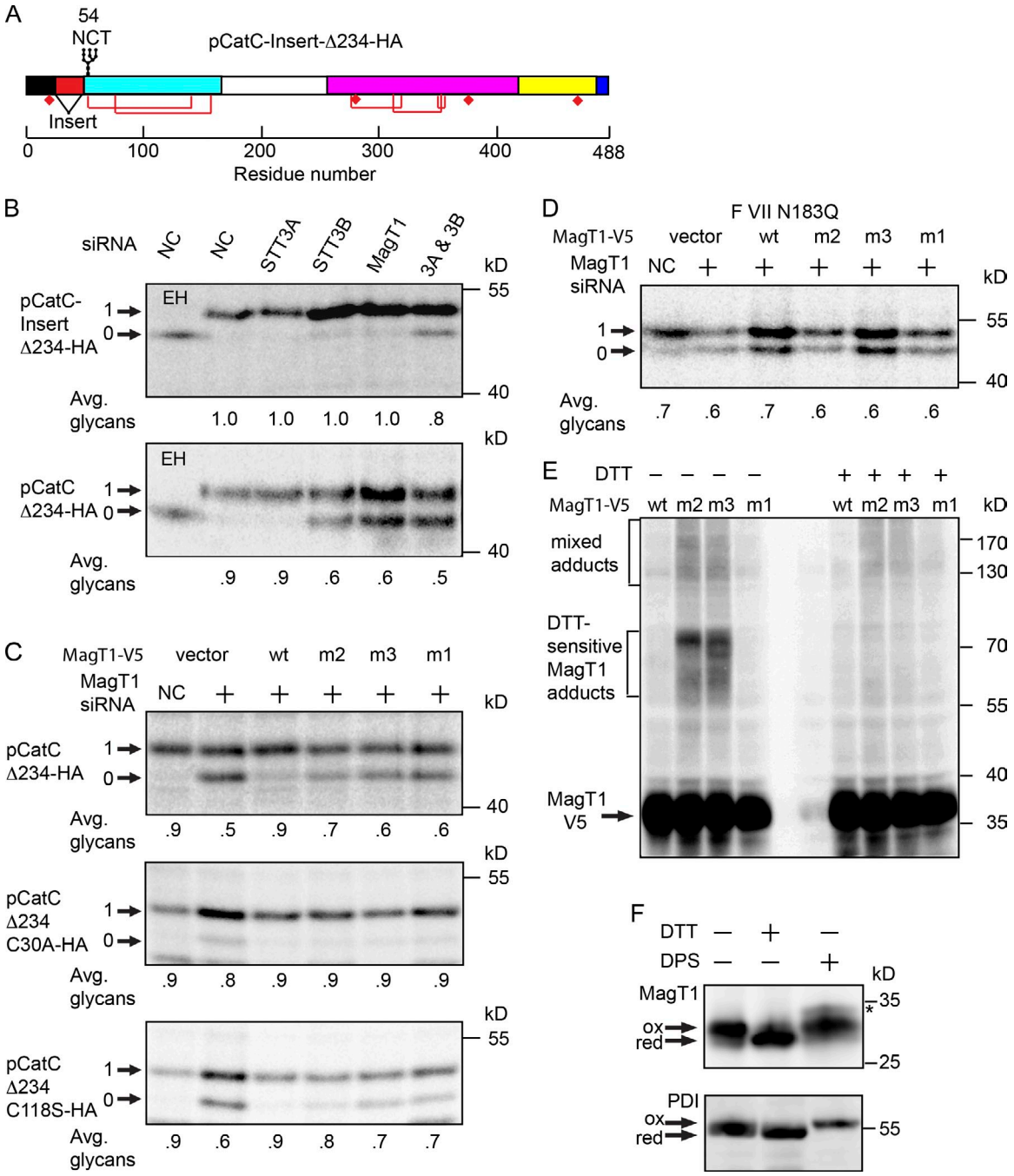

Figure 6. **Formation of mixed disulfides between MagT1 and glycoprotein substrates.** (A) Diagram of the pCatC-Insert-Δ234 construct. (B–D) HeLa cells were treated with the NC or MagT1 siRNA for 48 h before cotransfection with wild-type or mutant versions of the pCatCΔ234-HA (B and C), FVII N183Q (D), and MagT1-V5 expression vectors (B–D). The m1, m2, and m3 mutants of MagT1 are defined in Fig. 5 A. Cells were pulse labeled for 4 min (A–D) and chased for 10 min (B and C) or 40 min (D). Glycoproteins were immunoprecipitated with anti-HA sera (B and C) or anti-FVII sera (D) and quantified after SDS-PAGE. (E) Cells expressing wild-type or mutant versions of MagT1-V5 were treated with NEM to prevent disulfide exchange during cell lysis and sample preparation. Total cell extracts were resolved by nonreducing (−DTT) or reducing (+DTT) SDS-PAGE as indicated, and analyzed by protein immunoblotting using anti-V5 sera. (F) In vivo redox status of MagT1 and PDI in HeLa cells was assayed using a maleimide-shift protocol. The arrows designate oxidized and reduced forms of MagT1 and PDI. A minor MagT1 reactive band in the DPS-oxidized lane (asterisk) is probably due to inefficient formation of a disulfide between cysteine residues located on the cytoplasmic face of TM3 and TM4 (see Fig. 5 A for a map of MagT1 cysteine residues). Quantified values below gel lanes (B–D) are for the displayed image, which is representative of two experiments.

cysteine-containing site in pCatC? We inserted a 25-residue spacer sequence between the signal sequence cleavage site and the $N_{29}CT$ site (Fig. 6 A) to test whether proximity to the signal sequence favors site skipping by STT3A. Glycosylation of pCatC-Insert-Δ234-HA construct was completely insensitive to MagT1 or STT3B depletion but was sensitive to simultaneous, albeit partial, depletion of STT3A plus STT3B.

Two single site cysteine mutants of MagT1-V5 were constructed (Fig. 5 A, m2 and m3 mutants) to test whether the oxidized form of MagT1 is required for restoration of pCatCΔ234-HA

glycosylation. The MagT1 mutants and the pCatCΔ234-HA reporter construct were coexpressed in MagT1-depleted cells (Fig. 6 B). Remarkably, the m2 mutant (MagT1-V5 C87S) was more effective than the m3 mutant (MagT1-V5 C90S) or the double cysteine mutant in restoring glycosylation of pCatCΔ234-HA.

Two single-site cysteine mutants of pCatCΔ234-HA were constructed to determine whether one or both cysteine residues that form the C30-C118 disulfide in the substrate are critical for STT3B/MagT1-dependent glycosylation of the N_{29}CT site. Glycosylation of pCatCΔ234-HA C30A was efficient and showed no dependence upon the active site cysteine residues in MagT1 (Fig. 6 C). In contrast, glycosylation of pCatCΔ234-HA C118S remained MagT1 dependent, demonstrating that C30 can form a nonnative disulfide that interferes with glycosylation of the N_{29}CT site. As observed for pCatCΔ234-HA, the MagT1-V5 C87S mutant allowed near-normal glycosylation of pCatCΔ234-HA C118S. We next asked whether the MagT1-V5 mutants were able to promote glycosylation of the disulfide bracketed N_{360}IT site in factor VII. None of the MagT1-V5 cysteine mutants were active, which indicated that the oxidized form of MagT1 is necessary for promoting glycosylation of the N_{360}IT site in factor VII (Fig. 6 D).

Elimination of one of the active site cysteine residues in an oxidoreductase will stabilize mixed disulfide adducts. For example, when both active CXXC sites in the thioredoxin homologue ERp57 are replaced with CXXA, ERp57 forms stable mixed disulfides with nascent glycoproteins (Jessop et al., 2007). To determine whether the MagT1 mutants form mixed disulfides, intact HeLa cells expressing wild-type or mutant versions of MagT1 were treated with *N*-ethyl maleimide (NEM) to prevent disulfide bond formation or exchange after cell lysis. Cell extracts were resolved by nonreducing or reducing SDS-PAGE to separate MagT1 from potential MagT1-mixed disulfide adducts. Immunoblot analysis using antibodies to the V5 tag detected MagT1-V5 as well as higher molecular weight immunoreactive products (Fig. 6 E) ranging in size between 55 and 170 kD. The major adducts (55–75 kD) were DTT sensitive, hence they correspond to mixed disulfides between a MagT1 mutant and 25–40 kD proteins. The higher molecular weight adducts (>80 kD) included both DTT-sensitive and -insensitive MagT1 adducts. As expected, DTT-sensitive adducts were not formed in cells expressing wild-type MagT1 or the MagT1-V5 C87S C90S mutant, demonstrating that stabilized adduct formation is dependent on the presence of a single cysteine in the CXXC motif.

We used a previously described sequential cysteine alkylation procedure (Jessop and Bulleid, 2004) to probe the redox status of the catalytic cysteine residues in MagT1. Intact HeLa cells were (a) untreated; (b) incubated with dipyridyl disulfide (DPS), a cell-permeable oxidizing reagent; or (c) incubated with DTT, a cell-permeable reducing agent. The latter two treatments will, respectively, oxidize or reduce the CVVC motif in MagT1. Subsequent treatment of intact cells with NEM alkylates solvent exposed cysteine residues and blocked disulfide exchange reactions during cell lysis. Subsequent alkylation of the cell extracts with a higher molecular weight maleimide (4-acetamido-4′-malemidylstilbene-2,2′-disulfonic acid; AMS) in the presence of a thiol-free reducing agent (tris (2-carboxyethyl) phosphine; TCEP) allows resolution of the fully oxidized and reduced forms of MagT1 on an SDS-PAGE gel (Fig. 6 D). The majority of MagT1 from untreated cells co-migrated with DPS-oxidized MagT1, which indicates that the redox environment of the RER favors the oxidized CVVC motif. We also detected a less abundant reduced form of MagT1. PDI from untreated cells, which served as an internal control, mainly co-migrated with DTT-treated PDI, which is consistent with previous studies indicating that the fully reduced and semi-oxidized forms of PDI are the predominant forms in vivo (Jessop and Bulleid, 2004; Appenzeller-Herzog and Ellgaard, 2008).

Discussion

The cellular role of MagT1 and TUSC3 was controversial due to conflicting studies that these proteins are either magnesium transporters or OST subunits (Kelleher et al., 2003; Goytain and Quamme, 2005; Zhou and Clapham, 2009). Here we have presented evidence that MagT1 is a subunit of the STT3B isoform of the OST that is necessary for glycosylation of a subset of acceptor sites that are near cysteine residues. The CXXC motif in MagT1 and TUSC3 is required for function and is predominately in the oxidized state (Fig. 7 A). The previously described links between MagT1 or TUSC3 expression and magnesium ion homeostasis (Goytain and Quamme, 2005; Zhou and Clapham, 2009; Li et al., 2011) likely occur by an indirect mechanism involving glycosylation of a protein that is needed for Mg^{2+} transport activity.

Cotranslational glycosylation of acceptor sites in cysteine-rich protein domains

Native and nonnative disulfide bonds begin to form when the nascent polypeptide enters the oxidizing environment of the ER lumen (Bulleid and Ellgaard, 2011). For that reason, it is remarkable that MagT1 and TUSC3 exclusively assemble with the STT3B isoform of the OST (Fig. 7 A). Consistent with evidence that MagT1 and TUSC3 do not coprecipitate or copurify with STT3A (Kelleher et al., 2003; Shibatani et al., 2005), MagT1 is not required for glycosylation of STT3A-dependent substrates. Proteins that are strongly STT3A dependent (prosaposin and progranulin) are composed of small independent folding domains with multiple disulfides per repeat unit (Fig. S1, A and B). We conclude that cotranslational scanning of the nascent polypeptide by the translocation channel–associated STT3A complex allows efficient glycosylation of acceptor sites before disulfide bond formation in substrates that have a high density of cysteine residues (Fig. 7 B). When cotranslational glycosylation of progranulin or prosaposin is reduced by STT3A depletion, the STT3B isoform of the OST is not able to efficiently modify these sites despite the presence of MagT1, presumably because of the rapid formation of multiple disulfides that stabilize the small protein domains. Transferrin, another disulfide-rich protein that is cotranslationally glycosylated by STT3A (Shrimal et al., 2013b), has cysteine residue within five residues of both acceptor sites.

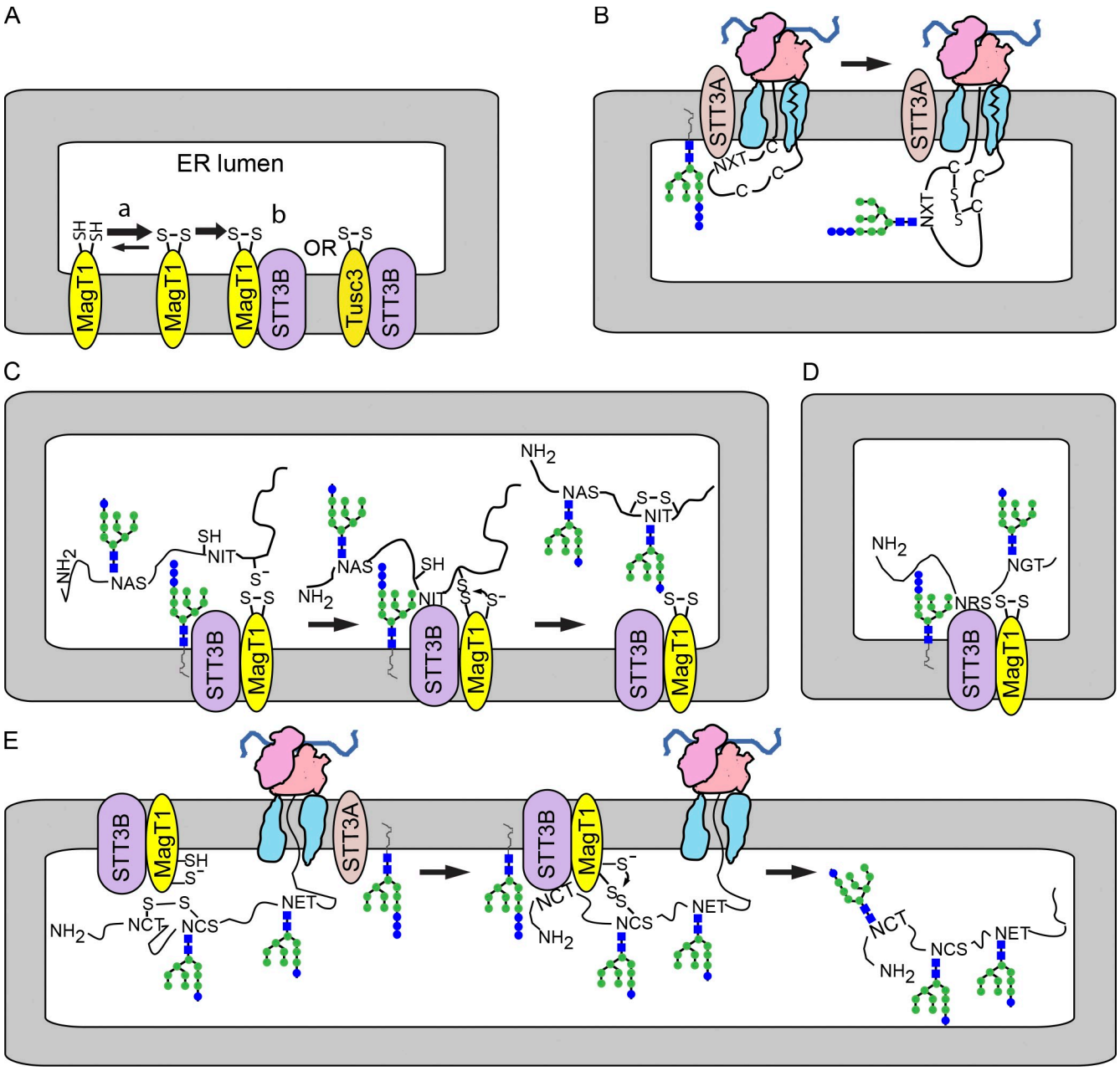

Figure 7. **MagT1-dependent glycosylation of sequons by the STT3B complex.** (A) MagT1 or TUSC3, primarily in the oxidized state, assemble into the STT3B complex. (B) Cotranslational glycosylation of sequons in cysteine-rich protein domains by the STT3A complex. (C) Formation of a transient mixed disulfide between MagT1 and a glycoprotein substrate facilitates posttranslocational glycosylation of a cysteine-proximal sequon by the STT3B complex. (D) MagT1 is required for full activity of the STT3B complex even when substrates lack nearby cysteine residues. (E) The reduced form of MagT1, perhaps generated in situ, can reduce a disulfide by forming a transient mixed disulfide.

Oxidoreductase activity of MagT1 and TUSC3

Both TUSC3 and MagT1 can be functionally incorporated into the STT3B complex (Fig. 7 A), which indicates that MagT1 and TUSC3 have overlapping functions in cells that express both proteins. Analysis of the role of MagT1 in glycosylation of factor VII and cathepsin C was particularly informative. The N_{360}IT site in factor VII is posttranslocationally glycosylated by an STT3B- and MagT1-dependent process (Fig. 7 C). Mutagenesis of the cysteine residues flanking the N_{360}IT site caused a slight reduction in skipping by STT3A, and accelerated the kinetics of posttranslocational glycosylation. Previous studies have shown that complete oxidation of the cysteine residues in factor VII lags behind glycosylation of the N_{360}IT site (Bolt et al., 2005; Ruiz-Canada et al., 2009). We propose that the oxidized CXXC motif in MagT1 reacts with a cysteine residue flanking the N_{360}IT site in factor VII (Fig. 7 C) to form a transient mixed disulfide. Mutagenesis of one or both cysteine residues in the CXXC motif of MagT1 blocked the ability of MagT1 to facilitate glycosylation of the N_{360}IT site in factor VII. After glycosylation, the substrate would be released from MagT1 by reaction of the free MagT1 thiol with the mixed disulfide

(Fig. 7 C). This should be the predominant reaction pathway for MagT1 in the cell.

Several lines of evidence indicate that glycosylation of the N_{29}CT site in pCatC involves reduction of a nonnative disulfide in pCatC by the reduced form of MagT1 (Fig. 7 E). Glycosylation of the N_{29}CT site in cathepsin C was MagT1 dependent unless C30 was replaced with an alanine residue or the ER lumen was reduced with DTT. Mutagenesis of C118, which forms the native disulfide with C30, did not eliminate the MagT1 dependence of N_{30}CT glycosylation. The C87S mutant of MagT1 stimulated glycosylation of the N_{29}CT site within both the context of pCatCΔ234-HA and pCatCΔ234-HA C118S, which suggests that C90 in MagT1 forms a mixed disulfide with pCatC upon reduction of a nonnative disulfide involving C30 and a second cysteine residue (Fig. 7 E). Importantly, formation of a mixed disulfide between C30 and MagT1 would not promote glycosylation, but would delay glycosylation by blocking entry of the sequon into the STT3B active site. Formation of mixed disulfides between MagT1 C87S and MagT1 C90S and HeLa cell proteins supports the conclusion that a reduced form of MagT1 can react with protein disulfides.

Role of yeast homologues of MagT1 in protein glycosylation

Yeast OST complexes have a single copy of Ost3p or Ost6p (Knauer and Lehle, 1999; Spirig et al., 2005). The active site CXXC motif of Ost6p is strongly reducing, hence Ost6p is thought to be fully oxidized in vivo (Schulz et al., 2009). Ost3p and Ost6p are required for efficient glycosylation of a subset of yeast acceptor sites that are on average closer to a cysteine residue in the substrate than sequons that are not Ost3p or Ost6p dependent (Schulz et al., 2009). Ost3p or Ost6p are proposed to form a mixed disulfide with a free cysteine residue in the nascent polypeptide as it enters the ER lumen, thereby delaying disulfide bond formation until STT3 can modify the cysteine-proximal sequons in the substrate (Schulz et al., 2009). Fungal STT3 proteins are more closely related to STT3B than STT3A (Shrimal et al., 2013b), which is consistent with exclusive assembly of MagT1 or TUSC3 into the STT3B complex.

Sequon skipping by STT3A correlates with MagT1 dependence

Here, we analyzed glycosylation of acceptor sites in seven human glycoproteins that have a total of 27 glycosylation sites located within 15 residues of the nearest cysteine residue (Fig. S1). Although glycosylation of only 7 of the 27 sites was dependent on STT3B and MagT1, proximity to a cysteine residue does not provide a reliable basis for predicting whether a sequon is MagT1 dependent.

Sequon skipping by the translocation channel–associated STT3A complex provides a far stronger basis for predicting whether a cysteine-proximal site is MagT1 dependent. The N_{29}CT site in pCatC and the N_{187}CS site in Hpx are examples of MagT1-dependent sites that have a cysteine residue as the X position. Even though cathepsin C has two sequons with internal cysteine residues, glycosylation of the N_{53}CS site in pCatC occurs by a MagT1 independent pathway. Why are certain NCT/S sites skipped by STT3A, while others are not? Our previous conclusion (Ruiz-Canada et al., 2009) that sequon skipping of the N_{29}CT site by the STT3A complex was caused by proximity to the signal sequence was verified by inserting a spacer segment that now allowed cotranslational glycosylation of the NCT site by STT3A. Cysteine 188 in Hpx (N_{187}CS site) forms a disulfide with a nearby cysteine residue (C200) in the folded protein (Fig. S1 C). The STT3B dependence of N187 glycosylation was greatly reduced by replacing the suboptimal NCS site with an NCT site (S188T mutation; Shrimal and Gilmore, 2013) due to a reduction in site skipping by STT3A.

Oxidoreductase-independent roles for the Ost3/Ost6 family

Extreme C-terminal sequons, which are skipped with high probability by the STT3A complex (Shrimal et al., 2013b), are MagT1 dependent in substrates that are bracketed by disulfides (Hpx and SHBG; Fig. S1, C and D) as well as substrates that lack nearby disulfides (β-GUS and the SHBG C362S C390S mutant; Fig. S2, B and C). Thus, MagT1 is required for the full activity of the STT3B complex even when the oxidoreductase activity is not required for glycosylation of a specific acceptor site (Fig. 7 D). Oxidoreductase-dependent and -independent roles for Ost3p and Ost6p in N-glycosylation have also been described previously (Schulz et al., 2009). TUSC3 has a hydrophobic peptide binding pocket near the active site that can accommodate a cysteine containing peptide in two orientations (Mohorko et al., 2014). This peptide-binding activity of the Ost3 protein family might be responsible for their oxidoreductase-independent role in N-glycosylation. Further experiments are needed to determine whether MagT1, by virtue of a peptide binding activity, directs glycoprotein substrates into the catalytic site of STT3B.

MagT1 and TUSC3 deficiencies cause milder forms of CDG-I than an STT3B deficiency

The *TUSC3* ARMR and *MAGT1* XLMR patients described to date do not have the wide spectrum of additional developmental and multiorgan abnormalities that are associated with CDG-I in general (Freeze and Aebi, 2005; Haeuptle and Hennet, 2009) or with STT3B-CDG (Shrimal et al., 2013a). Importantly, three TUSC3 ARMR patients in one consanguineous family have a homozygous nonsense mutation (Q55X) in the TUSC3 gene; therefore the less severe phenotype of TUSC3 ARMR relative to STT3B-CDG cannot be explained by a partial loss-of-function allele (Garshasbi et al., 2011). Hypoglycosylated variants of serum transferrin, the standard diagnostic marker for CDG-1, are not present in the serum of TUSC3 ARMR patients, nor are there alterations in the structure of protein-linked oligosaccharides (Molinari et al., 2008). However, serum transferrin is primarily synthesized by the liver, an organ that does not express TUSC3 (Molinari et al., 2008). Because transferrin is an STT3A-dependent substrate that was not hypoglycosylated by a patient with STT3B-CDG (Shrimal et al., 2013a,b), a MagT1 deficiency should also not cause hypoglycosylation of transferrin. For these reasons, there was no direct evidence that ARMR or

XLMR was caused by a defect in protein N-glycosylation or that these syndromes were related to CDG-1. The overlapping functions of MagT1 and TUSC3 likely explain why TUSC3-ARMR and MAGT1-XLMR patients have less severe clinical symptoms than the patient with STT3B-CDG (Shrimal et al., 2013a).

Protein glycosylation and disulfide bond formation can be viewed as competing reactions in the lumen of the ER because nascent polypeptides cease to be OST substrates upon acquiring a folded conformation. Efficient cotranslational glycosylation of sequons by the translocation channel–associated STT3A complex minimizes competition between disulfide bond formation and protein glycosylation even when sequons are located in cysteine-rich protein domains like those found in granulin, prosaposin, and transferrin. Here, we have shown that MagT1 and TUSC3 are oxidoreductases that exclusively assemble with the STT3B isoform of the OST to facilitate glycosylation of sequons that are skipped by the STT3A complex and are proximal to cysteine residues in the nascent glycoprotein. Together, these two mechanisms for mediating glycosylation of cysteine proximal sequons reduce competition between disulfide bond formation and N-glycosylation in metazoan glycoproteins.

Materials and methods

Protein expression vectors

Plasmids encoding MagT1 (NCBI NM_032121) and TUSC3 (NCBI NM_178234) were purchased from Integrated DNA Technologies. The MagT1 sequence was appended with a T7 epitope tag coding sequence followed by a stop codon and inserted into the pCMV6-AC-DDK-His vector (OriGene). The MagT1-V5-His vector was obtained by inserting the MagT1 sequence into the pCDNA4/V5-His A vector (Life Technologies) using the BamHI and XhoI cloning sites. The TUSC3 coding sequence was cloned into pCMV6-AC-DDK-His vector using the SgfI and MluI cloning sites. The STT3B-myc-DDK expression vector was purchased from OriGene. Site directed mutagenesis was used to replace cysteine residues in substrates, MagT1, or TUSC3 with serine or alanine residues as indicated. The MagT1 coding sequence was modified by PCR to create an siRNA-resistant MagT1-V5-His plasmid by introducing the underlined silent mutations 5′-AGCGTGATTGTGATGTTT-3′ in the region that includes the siRNA target sequence (5′-TCCGTTATCGTCATGTTC-3′).

The human SHBG coding sequence in pRC/CMV (Invitrogen) was provided by G. Hammond (Child and Family Research Institute, Vancouver, British Columbia, Canada; Bocchinfuso et al., 1992). The β-GUS expression vector (pCMV6 β-GUS-MycDDK) and a Hpx cDNA clone were purchased from OriGene. The Hpx coding sequence was cloned into the pCMV6-AC-DDK-His vector (OriGene). Glycosylation sites were eliminated by site-directed mutagenesis to obtain vectors to express β-GUS-Δ123-MycDDK (Shrimal et al., 2013b) and HpxΔ145-DDKHis (Shrimal and Gilmore, 2013). The expression vector for factor VII (pcDNA3-FVII) was modified by site-directed mutagenesis to obtain factor VII N183Q (Ruiz-Canada et al., 2009). A human cDNA clone for pCatC obtained from GE Healthcare (clone ID 2967491) was repaired to remove a 62-bp internal deletion, appended with the coding sequence for a C-terminal HA tag, and inserted into pcDNA3 to obtain pcDNA3-CatC-HA and pCatCΔ234-HA (Ruiz-Canada et al., 2009). DNA encoding residues 144–169 of pCatC (TASENVYVNTAHLKNSQEKYSNRLY) was inserted between T26 and P27 of pCatCΔ234-HA to create the pCatC-Insert-Δ234-HA plasmid.

Cell culture, plasmid, or siRNA transfection and pulse labeling of glycoproteins

HeLa cells (ATCC CCL-13) and primary skin fibroblasts were cultured as described previously (Shrimal et al., 2013a,b). Procedures for siRNA transfection were the same as described previously (Shrimal et al., 2013b) using the following concentrations of siRNA: negative control siRNA (NC) or STT3B, 60 nM; STT3A, MagT1, or TUSC3, 50 nM. The siRNAs specific for STT3A and STT3B have been characterized previously (Ruiz-Canada et al., 2009; Shrimal et al., 2013b). The STT3A siRNA is 5′-GGCCGUUUCUCUCACCGGCdTdT-3′ annealed with 5′-UCCGGUGAGAGAAACGGCCdTdT-3′. The STT3B siRNA is 5′-GCUCUAUAUGCAAUCAGUAdTdT-3′ annealed with 5′-CACUGAUUGCAUAUAGAGCdTdT-3′. TheMagT1siRNAis5′-CCGUUAUCGUCAUGUUCAUdTdT-3′ annealed with 5′-GUGAACAUGACGAUAACGGdTdT-3′. The TUSC3 siRNA is 5′-CCACGGCUAUCCUUAUAGUdTdT-3′ annealed with 5′-ACUAUAAGGAUAGCCGUGGdTdT-3′. siRNAs were ordered from GE Healthcare or Sigma-Aldrich. NC (#1027310) was purchased from QIAGEN.

Plasmid transfection was done after 48 h of siRNA treatment using 4–8 µg of plasmid and Lipofectamine 2000 in Opti-MEM (Gibco). The MagT1 complementation experiments were conducted by cotransfecting HeLa cells with the MagT1-V5 or TUSC3-DDK-His expression vector and the assay substrate expression vector (e.g., pCatCΔ123) 48 h after the cells were treated with the MagT1 siRNA.

Glycoprotein substrates in HeLa cells were pulse or pulse-chase labeled with Tran^{35}S label (PerkinElmer) as described previously (Shrimal et al., 2013a,b). In brief, cells were incubated in methionine- and cysteine-free DMEM media (Gibco) containing 10% dialyzed FBS for 20 min before the addition of 200 µCi/ml of Tran^{35}S label (PerkinElmer). Pulse-labeling periods were terminated by the addition of unlabelled methionine (3.75 mM) and cysteine (0.75 mM). Cells from one culture dish at each time point were lysed at 4°C by a 30-min incubation with 1 ml of RIPA lysis buffer. Lysates were clarified by centrifugation (2 min at 13,000 rpm) and precleared by incubation for 2 h with control IgG and a mixture of protein A/G Sepharose beads (Life Technologies) before an overnight incubation with protein or epitope tag–specific antibodies. Immunoprecipitates collected with protein A/G–Sepharose beads were washed five times with RIPA lysis buffer and twice with 10 mM Tris-HCl before eluting proteins with gel loading buffer. As indicated, immunoprecipitated proteins were digested with EH (New England Biolabs, Inc.). Dry gels were exposed to a phosphor screen (Fujifilm), scanned with a laser scanner (Typhoon FLA 9000; GE Healthcare), and quantified using Image Quant TL software (GE Healthcare). The pulse-chase data for factor VII glycosylation was fit to a single exponential equation using KaleidaGraph 3.6 (Synergy Software).

Cell surface biotinylation and protein immunoblotting

Cell-surface proteins were biotinylated as described previously (Bas et al., 2011). In brief, HeLa cells at 80% confluence were washed four times with ice-cold PBS. The cells were then incubated twice for 15 min on ice with 1 mg/ml EZ-link Sulfo-NHS-SS-Biotin (Thermo Fisher Scientific) in PBS. The biotinylation solution was removed and the cells were washed three times with quench solution (PBS containing 100 mM glycine) and incubated twice for 15 min on ice with fresh quench solution. After washing twice with PBS, cells were lysed with 1 ml of ice-cold RIPA lysis buffer containing protease inhibitors and centrifuged for 10 min at 13,000 rpm. Cell lysates containing 250 µg of protein were incubated overnight with 50 µl of NeutrAvidin Agarose resin (Thermo Fisher Scientific) equilibrated in RIPA buffer. The beads were washed three times with RIPA buffer, and proteins were eluted with SDS gel loading buffer. The entire eluate fraction and 20% of the input fraction were resolved by SDS-PAGE and analyzed by protein immunoblotting. Proteins were detected by protein immunoblotting as described previously (Kelleher et al., 2003) and quantified using Image Quant TL software (GE Healthcare). The percentage of cell surface exposed protein was calculated by dividing the biotinylated fraction value by the normalized total protein fraction value.

In vivo redox status of MagT1

The in vivo redox status of MagT1 was determined using a maleimide modification procedure (Jessop and Bulleid, 2004). In brief, 60-mm dishes of HeLa cells were either untreated or treated with either 10 mM DTT (Soltec Ventures) or 2 mM DPS (Alfa Aesar) in DMEM-FBS media for 5 min. The remaining free thiols were alkylated with 25 mM NEM (Sigma-Aldrich) in PBS for 20 min on ice. Cells were washed with ice-cold PBS and lysed in 700 µl of RIPA buffer in the presence of protease inhibitors. The lysates were denatured by heating for 20 min at 55°C in the presence of 1% SDS. To reduce existing disulfide bonds, TCEP (Thermo Fisher Scientific) was added up to 10 mM and the samples were incubated for 15 min at room temperature. 50 µl of each sample was adjusted to 30 mM AMS (Molecular Probes, Invitrogen) and incubated for 1 h at room temperature. Proteins were resolved by SDS-PAGE and detected by protein immunoblotting with antibodies specific for PDI and MagT1.

Native immunoprecipitation and mass spectrometry

Aliquots (100 µl) of rabbit IgG or anti-STT3B sera were incubated by end-over-end rotation for 18 h at 4°C with 500 µl of protein A–Sepharose beads in PBS. The beads were transferred to a 15-ml falcon tube and washed five times with 0.2 M triethanolamine-OAc, pH 7.5, to remove

unbound proteins. Protein A–bound IgG was immobilized by incubating with 25 mM disuccinimidyl suberate (Thermo Fisher Scientific) in 0.2 M triethanolamine-OAc, pH 7.5, at 4°C for 90 min followed by quenching with 50 mM Tris-Cl, pH 7.5. The conjugated beads were washed thoroughly and stored in 20 mM Tris-Cl, pH 7.5, and 150 mM NaCl at 4°C.

HeLa cells expressing MagT1-V5His were lysed at 4°C by a 30-min incubation with buffer A (20 mM Tris-Cl, pH 7.5, 150 mM NaCl, 5 mM $MgCl_2$, 3 mM $MnCl_2$, and 1× protease inhibitor cocktail [PIC; as defined in Kelleher et al., 1992]) plus 1.2% digitonin and DNase I. Cell lysates were clarified by centrifugation (10 min at 13,000 rpm). Precleared HeLa cell lysates or canine rough microsomes (10 µl, A_{280} = 50 in 1% SDS) were diluted in buffer A and were incubated for 16 h at 4°C with an antibody (anti-V5 or anti-STT3A) or IgG-conjugated beads. 60 µl of protein A/G–Sepharose beads were added to the samples containing nonconjugated antibodies and were further incubated for 4 h at 4°C. Beads were washed five times with buffer A containing 0.2% digitonin followed by two washes with 20 mM Tris-Cl, pH 7.5, and 150 mM NaCl. Washed beads were incubated in 80 µl of 20 mM Tris-Cl, pH 7.5, 150 mM NaCl, 1% Triton X-100, and 0.1% SDS at room temperature for 30 min to elute the proteins. Supernatants were collected by a brief centrifugation and proteins were resolved by SDS-PAGE. For mass spectrometry, eluates from immunoprecipitates were run ∼1 cm into a 10% SDS PAGE gel, and the entire protein-containing band was excised and sent to the University of Massachusetts Medical School proteomics and mass spectrometry core facility for LC-MS/MS.

Immunofluorescence

HeLa cells were cultured in Millicell EZ slides (EMD Millipore), washed in PBS, and fixed with 4% formaldehyde in PBS for 20 min. After permeabilization with 0.1% Tween-20 in PBS, cells were blocked in 5% goat serum (Sigma-Aldrich) in PBS for 30 min and incubated overnight with primary antibodies at a 1:100 dilution in the blocking buffer. Cells were then washed with blocking buffer and incubated for 1 h with secondary antibodies at a 1:200 dilution in the blocking buffer. The secondary antibodies were Alexa Fluor 488 goat anti–rabbit (A-11034; Molecular Probes; Life Technologies) and Alexa Fluor 594 goat anti–mouse (A-11032; Molecular Probes; Life Technologies). After rinsing with blocking buffer, cells were covered with Vectashield Mounting medium with DAPI (Vector Laboratories). Fluorescence images were acquired at room temperature with a confocal microscope (DM IRE2; Leica) using a 63×, 1.4 NA oil immersion objective lens (Leica) and Leica Confocal Software (V2.1).

Sources of antibodies

The rabbit antibody specific for STT3B was raised against recombinantly expressed N-terminal 73 residues of human STT3B as described previously (Ruiz-Canada et al., 2009). The rabbit polyclonal antibody against STT3A was raised against a synthetic peptide corresponding to the C terminus of human STT3A (residues 693–705) as described previously (Kelleher et al., 2003). The rabbit antibody to ribophorin I (RIC6; Yu et al., 1990) was raised against residues 564–583 of rat ribophorin I. The rabbit polyclonal antibody to OST48 was raised against a synthetic peptide corresponding to residues 437–445 of canine OST48 as described previously (Kelleher and Gilmore, 1997). Rabbit anti–saposin D was raised against recombinantly expressed human saposin D (residues 410–487 of human prosaposin) as described previously (Klein et al., 1994). The rabbit anti-Sec61α antibody was raised against a synthetic peptide corresponding to residues 463–476 of human Sec61α as described previously (Song et al., 2000).

Rabbit anti–human MagT1 (17430), rabbit anti–human TUSC3 (16039), and mouse anti–human glyceraldehyde 3-phosphate dehydrogenase (GAPDH; 60004) were obtained from Proteintech Group, Inc. Mouse anti–human BiP (610978) and mouse anti–human F_0F_1-ATP synthase α (612516) were from BD. The mouse anti–human STT3A antibody that was used for the native co-IP experiment was obtained from Abnova (ITM1, H00003703-M02). Goat anti–human cathepsin C (AF1071), goat anti–human factor VII (AF2338), goat anti–human progranulin (AF2420), and goat anti–human SHBG (AF2656) were purchased from R&D Systems. The mouse anti–human Na^+,K^+-ATPase α (ab7671) was from Abcam. Rabbit anti–human calreticulin (PA3-900) and mouse anti–rat PDI (MA3-019) were from Thermo Fisher Scientific. The rabbit anti–human malectin (SAB4200245) was obtained from Sigma-Aldrich. Rabbit IgG reagent (I-5006) was obtained from Sigma-Aldrich. The following antibodies against epitope tags were used: rabbit anti-T7 (PRB-186P; Covance), mouse anti-V5 (R96025; Life Technologies), rat anti-HA (11867423001; Roche), and mouse anti-DDK (F3165 anti-FLAG M2; Sigma-Aldrich).

Online supplemental material

Fig. S1 shows diagrams of the glycoprotein substrates used in this study. Fig. S2 shows that glycosylation of extreme C-terminal sites are STT3B and MagT1 dependent in a protein lacking disulfides (β-GUS) and in an SHBG derivative lacking cysteine residues near the acceptor sites. Fig. S3 presents evidence that HeLa cells do not express detectable amounts of endogenous TUSC3, and that exogenously expressed TUSC3-DDK can co-IP with STT3B. Online supplemental material is available at http://www.jcb.org/cgi/content/full/jcb.201404083/DC1.

We thank Scott Shaffer and Karin Green in the University of Massachusetts Medical School Proteomics and Mass Spectroscopy facility for the LC-MS/MS analysis of the co-IP experiments.

Research reported in this publication was supported by the National Institute of General Medical Sciences of the National Institutes of Health under award number GM43687.

The authors declare no competing financial interests.

Submitted: 15 April 2014
Accepted: 23 June 2014

References

Appenzeller-Herzog, C., and L. Ellgaard. 2008. In vivo reduction-oxidation state of protein disulfide isomerase: the two active sites independently occur in the reduced and oxidized forms. *Antioxid. Redox Signal.* 10:55–64. http://dx.doi.org/10.1089/ars.2007.1837

Bas, T., G.Y. Gao, A. Lvov, K.D. Chandrasekhar, R. Gilmore, and W.R. Kobertz. 2011. Post-translational N-glycosylation of type I transmembrane KCNE1 peptides: implications for membrane protein biogenesis and disease. *J. Biol. Chem.* 286:28150–28159. http://dx.doi.org/10.1074/jbc.M111.235168

Bocchinfuso, W.P., K.L. Ma, W.M. Lee, S. Warmels-Rodenhiser, and G.L. Hammond. 1992. Selective removal of glycosylation sites from sex hormone-binding globulin by site-directed mutagenesis. *Endocrinology*. 131:2331–2336.

Bolt, G., C. Kristensen, and T.D. Steenstrup. 2005. Posttranslational N-glycosylation takes place during the normal processing of human coagulation factor VII. *Glycobiology*. 15:541–547. http://dx.doi.org/10.1093/glycob/cwi032

Bulleid, N.J., and L. Ellgaard. 2011. Multiple ways to make disulfides. *Trends Biochem. Sci.* 36:485–492. http://dx.doi.org/10.1016/j.tibs.2011.05.004

Dumax-Vorzet, A., P. Roboti, and S. High. 2013. OST4 is a subunit of the mammalian oligosaccharyltransferase required for efficient N-glycosylation. *J. Cell Sci.* 126:2595–2606. http://dx.doi.org/10.1242/jcs.115410

Fetrow, J.S., N. Siew, J.A. Di Gennaro, M. Martinez-Yamout, H.J. Dyson, and J. Skolnick. 2001. Genomic-scale comparison of sequence- and structure-based methods of function prediction: does structure provide additional insight? *Protein Sci.* 10:1005–1014. http://dx.doi.org/10.1110/ps.49201

Freeze, H.H., and M. Aebi. 2005. Altered glycan structures: the molecular basis of congenital disorders of glycosylation. *Curr. Opin. Struct. Biol.* 15:490–498. http://dx.doi.org/10.1016/j.sbi.2005.08.010

Garshasbi, M., V. Hadavi, H. Habibi, K. Kahrizi, R. Kariminejad, F. Behjati, A. Tzschach, H. Najmabadi, H.H. Ropers, and A.W. Kuss. 2008. A defect in the TUSC3 gene is associated with autosomal recessive mental retardation. *Am. J. Hum. Genet.* 82:1158–1164. http://dx.doi.org/10.1016/j.ajhg.2008.03.018

Garshasbi, M., K. Kahrizi, M. Hosseini, L. Nouri Vahid, M. Falah, S. Hemmati, H. Hu, A. Tzschach, H.H. Ropers, H. Najmabadi, and A.W. Kuss. 2011. A novel nonsense mutation in TUSC3 is responsible for non-syndromic autosomal recessive mental retardation in a consanguineous Iranian family. *Am. J. Med. Genet. A.* 155A:1976–1980. http://dx.doi.org/10.1002/ajmg.a.34077

Goytain, A., and G.A. Quamme. 2005. Identification and characterization of a novel mammalian Mg^{2+} transporter with channel-like properties. *BMC Genomics*. 6:48. http://dx.doi.org/10.1186/1471-2164-6-48

Haeuptle, M.A., and T. Hennet. 2009. Congenital disorders of glycosylation: an update on defects affecting the biosynthesis of dolichol-linked oligosaccharides. *Hum. Mutat.* 30:1628–1641. http://dx.doi.org/10.1002/humu.21126

Jessop, C.E., and N.J. Bulleid. 2004. Glutathione directly reduces an oxidoreductase in the endoplasmic reticulum of mammalian cells. *J. Biol. Chem.* 279:55341–55347. http://dx.doi.org/10.1074/jbc.M411409200

Jessop, C.E., S. Chakravarthi, N. Garbi, G.J. Hämmerling, S. Lovell, and N.J. Bulleid. 2007. ERp57 is essential for efficient folding of glycoproteins sharing common structural domains. *EMBO J.* 26:28–40. http://dx.doi.org/10.1038/sj.emboj.7601505

Kelleher, D.J., and R. Gilmore. 1997. DAD1, the defender against apoptotic cell death, is a subunit of the mammalian oligosaccharyltransferase. *Proc. Natl. Acad. Sci. USA*. 94:4994–4999. http://dx.doi.org/10.1073/pnas.94.10.4994

Kelleher, D.J., and R. Gilmore. 2006. An evolving view of the eukaryotic oligosaccharyltransferase. *Glycobiology*. 16:47R–62R. http://dx.doi.org/10.1093/glycob/cwj066

Kelleher, D.J., G. Kreibich, and R. Gilmore. 1992. Oligosaccharyltransferase activity is associated with a protein complex composed of ribophorins I and II and a 48 kd protein. *Cell*. 69:55–65. http://dx.doi.org/10.1016/0092-8674(92)90118-V

Kelleher, D.J., D. Karaoglu, E.C. Mandon, and R. Gilmore. 2003. Oligosaccharyltransferase isoforms that contain different catalytic STT3 subunits have distinct enzymatic properties. *Mol. Cell*. 12:101–111. http://dx.doi.org/10.1016/S1097-2765(03)00243-0

Klein, A., M. Henseler, C. Klein, K. Suzuki, K. Harzer, and K. Sandhoff. 1994. Sphingolipid activator protein D (sap-D) stimulates the lysosomal degradation of ceramide in vivo. *Biochem. Biophys. Res. Commun.* 200:1440–1448. http://dx.doi.org/10.1006/bbrc.1994.1612

Knauer, R., and L. Lehle. 1999. The oligosaccharyltransferase complex from *Saccharomyces cerevisiae*. Isolation of the OST6 gene, its synthetic interaction with OST3, and analysis of the native complex. *J. Biol. Chem.* 274:17249–17256. http://dx.doi.org/10.1074/jbc.274.24.17249

Kowarik, M., S. Numao, M.F. Feldman, B.L. Schulz, N. Callewaert, E. Kiermaier, I. Catrein, and M. Aebi. 2006. N-linked glycosylation of folded proteins by the bacterial oligosaccharyltransferase. *Science*. 314:1148–1150. http://dx.doi.org/10.1126/science.1134351

Li, F.Y., B. Chaigne-Delalande, C. Kanellopoulou, J.C. Davis, H.F. Matthews, D.C. Douek, J.I. Cohen, G. Uzel, H.C. Su, and M.J. Lenardo. 2011. Second messenger role for Mg^{2+} revealed by human T-cell immunodeficiency. *Nature*. 475:471–476. http://dx.doi.org/10.1038/nature10246

Lizak, C., S. Gerber, S. Numao, M. Aebi, and K.P. Locher. 2011. X-ray structure of a bacterial oligosaccharyltransferase. *Nature*. 474:350–355. http://dx.doi.org/10.1038/nature10151

MacGrogan, D., A. Levy, G.S. Bova, W.B. Isaacs, and R. Bookstein. 1996. Structure and methylation-associated silencing of a gene within a homozygously deleted region of human chromosome band 8p22. *Genomics*. 35:55–65. http://dx.doi.org/10.1006/geno.1996.0322

Mohorko, E., R.L. Owen, G. Malojčić, M.S. Brozzo, M. Aebi, and R. Glockshuber. 2014. Structural basis of substrate specificity of human oligosaccharyl transferase subunit N33/Tusc3 and its role in regulating protein N-glycosylation. *Structure*. 22:590–601. http://dx.doi.org/10.1016/j.str.2014.02.013

Molinari, F., F. Foulquier, P.S. Tarpey, W. Morelle, S. Boissel, J. Teague, S. Edkins, P.A. Futreal, M.R. Stratton, G. Turner, et al. 2008. Oligosaccharyltransferase-subunit mutations in nonsyndromic mental retardation. *Am. J. Hum. Genet.* 82:1150–1157. http://dx.doi.org/10.1016/j.ajhg.2008.03.021

Nilsson, I., D.J. Kelleher, Y. Miao, Y. Shao, G. Kreibich, R. Gilmore, G. von Heijne, and A.E. Johnson. 2003. Photocross-linking of nascent chains to the STT3 subunit of the oligosaccharyltransferase complex. *J. Cell Biol.* 161:715–725. http://dx.doi.org/10.1083/jcb.200301043

Qin, S.Y., D. Hu, K. Matsumoto, K. Takeda, N. Matsumoto, Y. Yamaguchi, and K. Yamamoto. 2012. Malectin forms a complex with ribophorin I for enhanced association with misfolded glycoproteins. *J. Biol. Chem.* 287:38080–38089. http://dx.doi.org/10.1074/jbc.M112.394288

Roboti, P., and S. High. 2012. Keratinocyte-associated protein 2 is a bona fide subunit of the mammalian oligosaccharyltransferase. *J. Cell Sci.* 125:220–232. http://dx.doi.org/10.1242/jcs.094599

Ruiz-Canada, C., D.J. Kelleher, and R. Gilmore. 2009. Cotranslational and posttranslational N-glycosylation of polypeptides by distinct mammalian OST isoforms. *Cell*. 136:272–283. http://dx.doi.org/10.1016/j.cell.2008.11.047

Schallus, T., C. Jaeckh, K. Fehér, A.S. Palma, Y. Liu, J.C. Simpson, M. Mackeen, G. Stier, T.J. Gibson, T. Feizi, et al. 2008. Malectin: a novel carbohydrate-binding protein of the endoplasmic reticulum and a candidate player in the early steps of protein N-glycosylation. *Mol. Biol. Cell*. 19:3404–3414. http://dx.doi.org/10.1091/mbc.E08-04-0354

Schallus, T., K. Fehér, U. Sternberg, V. Rybin, and C. Muhle-Goll. 2010. Analysis of the specific interactions between the lectin domain of malectin and diglucosides. *Glycobiology*. 20:1010–1020. http://dx.doi.org/10.1093/glycob/cwq059

Schulz, B.L., C.U. Stirnimann, J.P. Grimshaw, M.S. Brozzo, F. Fritsch, E. Mohorko, G. Capitani, R. Glockshuber, M.G. Grütter, and M. Aebi. 2009. Oxidoreductase activity of oligosaccharyltransferase subunits Ost3p and Ost6p defines site-specific glycosylation efficiency. *Proc. Natl. Acad. Sci. USA*. 106:11061–11066. http://dx.doi.org/10.1073/pnas.0812515106

Shibatani, T., L.L. David, A.L. McCormack, K. Frueh, and W.R. Skach. 2005. Proteomic analysis of mammalian oligosaccharyltransferase reveals multiple subcomplexes that contain Sec61, TRAP, and two potential new subunits. *Biochemistry*. 44:5982–5992. http://dx.doi.org/10.1021/bi047328f

Shrimal, S., and R. Gilmore. 2013. Glycosylation of closely spaced acceptor sites in human glycoproteins. *J. Cell Sci.* 126:5513–5523. http://dx.doi.org/10.1242/jcs.139584

Shrimal, S., B.G. Ng, M.E. Losfeld, R. Gilmore, and H.H. Freeze. 2013a. Mutations in STT3A and STT3B cause two congenital disorders of glycosylation. *Hum. Mol. Genet.* 22:4638–4645. http://dx.doi.org/10.1093/hmg/ddt312

Shrimal, S., S.F. Trueman, and R. Gilmore. 2013b. Extreme C-terminal sites are posttranslocationally glycosylated by the STT3B isoform of the OST. *J. Cell Biol.* 201:81–95. http://dx.doi.org/10.1083/jcb.201301031

Song, W., D. Raden, E.C. Mandon, and R. Gilmore. 2000. Role of Sec61α in the regulated transfer of the ribosome-nascent chain complex from the signal recognition particle to the translocation channel. *Cell*. 100:333–343. http://dx.doi.org/10.1016/S0092-8674(00)80669-8

Spirig, U., D. Bodmer, M. Wacker, P. Burda, and M. Aebi. 2005. The 3.4-kDa Ost4 protein is required for the assembly of two distinct oligosaccharyltransferase complexes in yeast. *Glycobiology*. 15:1396–1406. http://dx.doi.org/10.1093/glycob/cwj025

Yu, Y.H., D.D. Sabatini, and G. Kreibich. 1990. Antiribophorin antibodies inhibit the targeting to the ER membrane of ribosomes containing nascent secretory polypeptides. *J. Cell Biol.* 111:1335–1342. http://dx.doi.org/10.1083/jcb.111.4.1335

Zhou, H., and D.E. Clapham. 2009. Mammalian MagT1 and TUSC3 are required for cellular magnesium uptake and vertebrate embryonic development. *Proc. Natl. Acad. Sci. USA*. 106:15750–15755. http://dx.doi.org/10.1073/pnas.0908332106